A UNIQUE FORMULATION OF PIECEWISE EXACT METHOD TO ANALYZE A NONLINEAR SPRING SYSTEM UNDER HARMONIC EXCITATION

P.-S. Xie

School of Civil and Transportation Engineering
Guangdong University of Technology
Guangzhou, China

P.-J. Shih *

Department of Civil and Environmental Engineering
National University of Kaohsiung
Kaohsiung, Taiwan

ABSTRACT

This paper introduces a unique, efficient, and exact formulation for solving a single-degree-of-freedom system with nonlinear stiffness under a harmonic loading. This formulation is one kind of the piecewise exact method, and its benefit lies in providing the closed-form exact solution in each displacement segment. Since the exact solution is given in each segment, the continuity between two segments can be confirmed. Consequently, no instability errors affect the analysis. To determine the exact solutions in these segments, this research develops a technique that shifts the equilibrium points of the piecewise linear segments, which are discretized from a nonlinear stiffness curve, to new equilibrium points in order to satisfy the typical linear exact solution. Thus, positive- and negative-stiffness linear segments can be solved with this technique. This formulation saves roughly 60% of the calculation time (error < 10^{-10}) as compared to the numerical approximation.

Keywords: Piecewise exact method, Nonlinear spring, Step-by-step procedure, The newmark explicit method.

1. INTRODUCTION

This paper introduces a unique, efficient, and exact formulation for solving a single-degree-of-freedom (SDOF) system with nonlinear stiffness under a harmonic loading. This method is a new formulation of the piecewise exact method (PEM). The typically dynamic solutions are applied, and a technique is introduced for shifting the equilibrium points to fit these solutions and develop this formulation. The appeal of the PEM lies in the fact that it provides the closed-form exact solution at each step, and thus it avoids many incorrect results caused by error propagation. No problems of instability errors occur in this formulation, which is practically better than numerical approximations.

The PEM is an elegant method for solving nonlinear systems, but there are few formulations of it. Clough and Penzien [1] classified the step-by-step procedures for solving nonlinear dynamic responses as either PEMs or numerical approximations. The merit of the PEM lies in the closed-form exact solution. The exact solutions are obtained directly from the equation of motion, and it shows the exact dynamics in each step-by-step procedures. And in the fact that the accuracy of the solutions is perfectly controlled with a sufficiently sized step, that the sized steps are determined by the discretization of the nonlinear curves before any iterations. Note that the only way to deal with the nonlinear is by applying discretization it into linear counterparts, if the nonlinearity cannot be written as a certainly continuous function. To the authors' knowledge, the reported formulations of the PEM are based on the time-intervals, and most of them are either the nonlinear loading system or the nonlinear spring system. A basic application of the PEM is a SDOF system including a constant spring property under a nonlinear loading history [1]. This system is also considered a linear hysteretic model, and the loading time history is composed of piecewise linear segments based on the time-intervals. From this technique, a bilinear spring property of the SDOF system [2] and a bilinear spring property of a multi-degree-of-freedom (MDOF) system [3] were developed. Clearly, not many models have been developed, but all formulations have been simple and elegant.

In this paper, a new PEM formulation is provided that is distinctly different from the previous PEMs (comparison shown on Table 1). This formulation controls the displacement segments instead of the time-steps, so that the times at the turning points between two segments become unknown but the displacements are given. This new concept focusing on displacement-steps of PEM has never been discussed in other literatures. Besides, to increase accuracy, it requires small sizes of segments to fit the nonlinearity but it increases number of turning points. The PEM exactly solves the instability problem raised at the turning points. To increase accuracy, it requires small sizes of segments to fit the nonlinearity but it increases number of turning points. The PEM exactly solves the

* Corresponding author (pjshih@nuk.edu.tw)

DOI : 10.1017/jmech.2014.83
Copyright © 2014 The Society of Theoretical and Applied Mechanics, R.O.C.
https://doi.org/10.1017/jmech.2014.83 Published online by Cambridge University Press

Table 1 The reported piecewise exact methods.

Resources	DOF	Step	Stiffness	Excitation force	Remarks
Clough and Penzien [1]	SDOF	Time	Linear	Piecewise polynomial	Basic type
Liu [2]	MDOF	Time	Bilinear hysteresis	Piecewise polynomial	Earthquake engineering (Duhamel integral used)
Aydinoglu and Fahjan [3]	SDOF	Time	Bilinear hysteresis	Piecewise polynomial	Earthquake engineering
The proposed formulation	SDOF	Displacement	Piecewise polynomial	Harmonic time history	Mechanic engineering MDOF application [4,5]

instability problem raised at the turning points. Furthermore, when this formulation is combined with the separation of variables method, the formulation can be expanded to solve an MDOF system. The displacement-step concept of this formulation was originally developed by the authors' MDOF models for solving contact vibration problem [4] and atomic force microscopy (AFM) vibration problem [5]. In the previous study [4], the contact boundary conditions of the Euler cantilever beam were considered with a single positive spring constant. In the study [5], nonlinear atomic force as the boundary condition, single positive spring constant, and only the attractive force were considered. Different from the nonlinear boundary conditions, the presented version develops the technique of shifting the equilibrium points for dealing with the nonlinear stiffness problem. It lets this formulation be applied to both positive and negative stiffness cases.

In addition to the PEM is an elegant method, the authors have adopted the PEM because conventional numerical approximation suffers from balancing between increasing accuracy and saving time. The numerical approximation procedure can be used as either an explicit method, such as the Newmark method [6], the Wilson-θ method [7], and the Houbolt scheme [8], or as an implicit method, such as the central difference scheme. Unfortunately, the accuracy of a numerical approximation cannot be a criterion for method selection. Although round-off and truncation errors can be overcome if high-digital-precision methods are applied in the calculation, instability errors occur when estimating time-steps or at the turning points between two segments [1]. These also result in errors propagating over several iterations. While any desired degree of accuracy can be obtained by any method if the time-step size is short enough to provide an adequate definition of the loading and the response, this will obviously correspond to increasing computational costs. Extensive research has focused on obtaining solutions that depend upon how an appropriate time-step is found [9-11] and what step-by-step integration method is used in the overall procedure [12,13]. Thus, convergence and accuracy depend on researchers' experiments or on simple trial and error.

This paper provides a unique formulation of the PEM, that is efficient and accurate compared to numerical approximation, for the case of a nonlinear spring system under harmonic excitation. Section 2 introduces the typical exact solutions of the piecewise segments, and we develop a technique to shift the equilibrium points of the system in order to deal with non-typical piecewise segments. Section 3 compares the proposed formulation and the Newmark explicit method. The advantages of the proposed formulation with respect to the Newmark explicit method are shown in relation to continuity at the turning points, error propagation (instability), and the issue of choosing an appropriate time-step.

2. THEORETICAL MODELS

The entire mass m of the system is included in a rigid block, which is constrained by rollers so that it can move only in simple translation. Thus, the single displacement coordinate u completely defines its position. The elastic resistance to displacement is determined by a weightless spring of nonlinear stiffness $k(u)$, while the energy loss mechanism is represented by the damper c. The external dynamic loading producing the response of this system is the time-varying force $f = p_0 \sin\omega t$, in which p_0 and ω are the amplitude and excitation frequency of the harmonic force, respectively. A sketch of the SDOF system is shown in Fig. 1.

The equation of motion is an expression of the equilibrium of these forces

$$m\ddot{u} + c\dot{u} + ku = p_0 \sin\omega t \tag{1}$$

where u, $\dot{u}$, and $\ddot{u}$ are the displacement, velocity, and acceleration of the system, respectively. In the following derivation, the nonlinear spring is divided into displacement segments, usually discretized by significant changes of slope in the actual spring property. It is assumed that the slope of the stiffness curve remains constant between two turning points, giving piecewise linear segments. Spring constants with positive and negative values are considered.

2.1 Exact Solution for the Positive Stiffness Model in a Segment

For the case where the spring stiffness is positive, divide Eq. (1) by m, giving

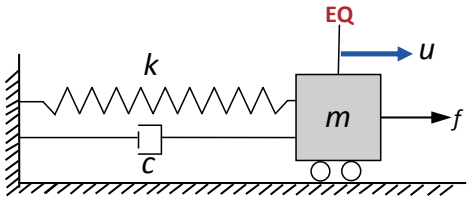


Fig. 1 A sketch of the SDOF system containing a rigid block, a nonlinear spring, and a damper.

https://doi.org/10.1017/jmech.2014.83 Published online by Cambridge University Press

$$\ddot{u} + 2\zeta\omega_n \dot{u} + \omega_n^2 u = p_0 \sin\omega t / m \tag{2}$$

in which the natural frequency is defined by $\omega_n = \sqrt{k/m}$, the damping coefficient $\zeta = c / 2m\omega_n$, and the damped frequency $\omega_D = \omega_n\sqrt{1-\zeta^2}$. Then the particular solution of Eq. (2) is defined by

$$u_p(t) = C\sin\omega t + D\cos\omega t \tag{3}$$

in which the coefficients C and D are obtained

$$C = (p_0/k)\left[1-(\omega/\omega_n)^2\right] / \left\{\left[1-(\omega/\omega_n)^2\right]^2 + \left[2\zeta(\omega/\omega_n)\right]^2\right\} \tag{4}$$

$$D = (p_0/k)\left[-2\zeta(\omega/\omega_n)\right] / \left\{\left[1-(\omega/\omega_n)^2\right]^2 + \left[2\zeta(\omega/\omega_n)\right]^2\right\} \tag{5}$$

Furthermore, the complementary solution of Eq. (2) at the initial time t_0 is

$$u_C(t) = e^{-\zeta\omega_n(t-t_0)}\left\{A\cos\left[\omega_D(t-t_0)\right] + B\sin\left[\omega_D(t-t_0)\right]\right\} \tag{6}$$

Then the total solution of Eq. (2) becomes

$$\begin{aligned} u(t) = {} & e^{-\zeta\omega_n(t-t_0)}\left\{A\cos\left[\omega_D(t-t_0)\right] + B\sin\left[\omega_D(t-t_0)\right]\right\} \\ & + C\sin\omega t + D\cos\omega t \end{aligned} \tag{7}$$

The last two terms don't shift the time because they are based on the global time system. Moreover, the velocity of the system is obtained

$$\begin{aligned} \dot{u}(t) = {} & -\zeta\omega_n e^{-\zeta\omega_n(t-t_0)}\left\{A\cos\left[\omega\omega t_D(t-t_0)\right]\right. \\ & \left. + B\sin\left[\omega_D(t-t_0)\right]\right\} \\ & + e^{-\zeta\omega_n(t-t_0)}\left\{-A\omega_D\sin\left[\omega_D(t-t_0)\right]\right. \\ & \left. + B\omega_D\cos\left[\omega_D(t-t_0)\right]\right\} \\ & + C\omega\cos\omega t - D\omega\sin\omega t \end{aligned} \tag{8}$$

In the above equations, the values of A and B depend on the conditions under which the response is initiated. Let the initial conditions of the system be $u(t_0) = u_0$ and $\dot{u}(t_0) = \dot{u}_0$ at a time $t = t_0$. Then A and B can be obtained

$$A = u_0 - C\sin\omega t_0 - D\cos\omega t_0 \tag{9}$$

$$B = (\dot{u}_0 + \zeta\omega_n A - C\omega\cos\omega t_0 + D\omega\sin\omega t_0)/\omega_D \tag{10}$$

Finally, the solution of Eq. (7) represents the oscillation in the certain displacement-interval under given initial conditions.

Figure 2(a) demonstrates the displacement-force relationship of the typical mass-spring model for the positive stiffness case. The rigid block periodically vibrates around the equilibrium point (EQ) with a displacement u' ($u' = u$), and the spring force always pulls the rigid block backward to the equilibrium point. Figure 2(b) shows the case that is a piecewise line with

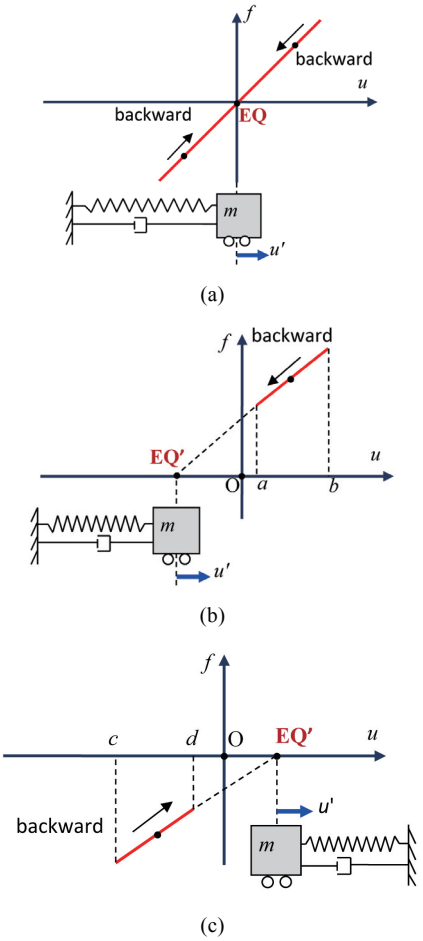


Fig. 2 Three types of the positive stiffness case; all spring forces pull the rigid blocks backward to the equilibrium points. The displacement-force curve lies on (a) the typical segment, and the equilibrium point at the origin; (b) the first quadrant segment, with oscillation defined in [a, b] and the equilibrium point shifting to EQ′; and (c) the third quadrant segment, with oscillation defined in [c, d] and the equilibrium point shifting to EQ′.

a passive stiffness in the interval [a, b], but its extended line does not run cross the origin O, in contrast to the previous EQ at O in Fig. 2(a). This shows that the new equilibrium point shifts to EQ′, which is a cross point of the extended line and u-axis. Instead of the real displacement u, the value u' measured from EQ′ is the amplitude of the new system. The local coordinate system u' helps to solve the exact response in each segment by applying Eqs. (7) and (8); the global coordinate system u, transformed from u', represents the real response of the system. On the other hand, Fig. 2(c) shows the piecewise line in the third quadrant. The equilibrium point has shifted to EQ′, and the amplitude u' is measured from EQ′ for the interval [c, d].

2.2 Exact Solution for the Negative Stiffness Model in a Segment

For the case of negative spring stiffness, dividing Eq. (1) by m gives

https://doi.org/10.1017/jmech.2014.83 Published online by Cambridge University Press

$$\ddot{u} + (c/m)\dot{u} + \omega_n' u = p_0 \sin \omega t / m \tag{11}$$

where $\omega_n' = k/m$. The particular solution of Eq. (11) is

$$u_p(t) = C' \sin \omega t + D' \cos \omega t \tag{12}$$

where the coefficients C and D are

$$C' = (p_0/k)\left[1-(\omega^2/\omega_n')\right] / \left[(1-\omega^2/\omega_n')^2 + (c\omega/k)^2\right] \tag{13}$$

$$D' = -(p_0\, c\omega/k^2) / \left[(1-\omega^2/\omega_n')^2 + (c\omega/k)^2\right] \tag{14}$$

The complementary solution of Eq. (11) is

$$u_C(t) = e^{-c(t-t_0)/2m}\left\{A' \cosh\left[\omega_D'(t-t_0)\right] + B' \sinh\left[\omega_D'(t-t_0)\right]\right\} \tag{15}$$

where t_0 is the initial time and $\omega_D' = \sqrt{(c/2m)^2 - k/m}$. The total solution is

$$u(t) = e^{-c(t-t_0)/2m}\left\{A' \cosh\left[\omega_D'(t-t_0)\right] + B' \sinh\left[\omega_D'(t-t_0)\right]\right\} + C' \sin \omega t + D' \cos \omega t \tag{16}$$

Then the velocity of the oscillation system is

$$\dot{u}(t) = (-c/2m)e^{-c(t-t_0)/2m}\left\{A' \cosh\left[\omega_D'(t-t_0)\right] + B' \sinh\left[\omega_D'(t-t_0)\right]\right\} + e^{-c(t-t_0)/2m}\omega_D'\left\{A' \sinh\left[\omega_D'(t-t_0)\right] + B' \cosh\left[\omega_D'(t-t_0)\right]\right\} + C'\omega \cos \omega t - D'\omega \sin \omega t \tag{17}$$

Substituting the initial conditions, $u(t_0) = u_0$ and $\dot{u}(t_0) = \dot{u}_0$, into Eqs. (16) and (17) gives

$$A' = u_0 - C' \sin \omega t_0 - D' \cos \omega t_0 \tag{18}$$

$$B' = \left[\dot{u}_0 + (c/2m)A' - C'\omega \cos \omega t_0 + D'\omega \sin \omega t_0\right] / \omega_D' \tag{19}$$

Finally, the solution of Eq. (15) represents the oscillation in a certain displacement-interval under the given initial conditions.

Unlike the positive stiffness case, the spring force pushes the rigid block far away from the equilibrium point. Figure 3(a) demonstrates a typical mass-spring model with the equilibrium point EQ at the origin O. The displacement u' is measured from EQ, and the spring force pushes the rigid block forward to leave EQ. In Fig. 3(b), a piecewise linear segment with negative stiffness is defined in the interval $[a,b]$, and its extended line runs crosses the u-axis at EQ′. The amplitude u' is measured from EQ′, which can be exactly obtained by Eq. (16). Thus, while the rigid block oscillates into this interval $[a,b]$, the instantaneous displacement and velocity at the entering moment, exactly solved from the previous segment, are used as the initial conditions in this segment. They should be transformed to the u' coordinate system. Similarly, Fig. 3(c) shows the piecewise linear segment in the third quadrant. The equilibrium point at EQ′ and new amplitude u' are shown for the interval $[c,d]$.

2.3 Continuity Between Two Piecewise Linear Segments

According to Eqs. (7) and (16), while the initial conditions at the turning point between two segments are given, the exact response of the oscillation can be obtained in the certain interval. The initial conditions also represent the continuity conditions at the turning points between the two segments, $u^{(N-1)}(t_0) = u^{(N)}(t_0)$ and $\dot{u}^{(N-1)}(t_0) = \dot{u}^{(N)}(t_0)$. Here, the displacement $u^{(N)}(t_0)$

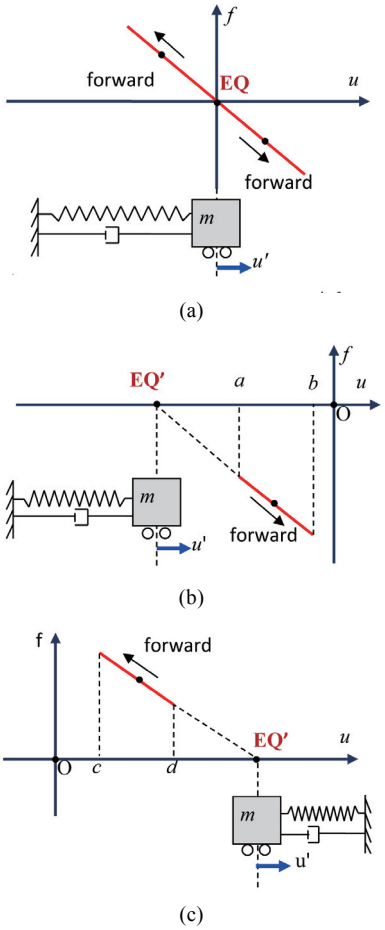


Fig. 3 Three types of the negative stiffness case; all spring forces push the rigid blocks to move from the equilibrium points. The displacement-force curve lies on (a) the typical segment and equilibrium point at the origin; (b) the third quadrant segment, with oscillation defined in [a, b] and the equilibrium point shifting to EQ′; and (c) the first quadrant segment, with oscillation defined in [c, d] and the equilibrium point shifting to EQ′.

https://doi.org/10.1017/jmech.2014.83 Published online by Cambridge University Press

is known according to the boundary of the displacement-interval. t_0 can be solved numerically by giving the initial displacement $u^{(N)}(t_0)$ in the inverse function of Eqs. (7) or (16). The velocity $\dot{u}^{(N)}(t_0)$ can be obtained from the previous segment if the turning point time is substituted in Eqs. (8) or (17). As a result, the continuity at the turning point is confirmed, solving the problem of instability in the step-by step procedure. Additionally, errors occurring from the calculation of t_0 can be estimated. The issue of how to select an appropriate time-step, although necessary in a conventional approximation problem, is not a factor in this formulation.

3. NUMERICAL ANALYSIS AND DISCUSSION

The numerical analysis demonstrates oscillation responses based on three kinds of stiffness curves: The positive case, the negative case, and the mixed positive and negative case. The parameters of the SDOF model are set as m = 0.2533 [lb], c = 0.1592 [lb/s], p_0 = 10 [kip], and $\omega = 5\pi/3$ [rad/sec] for all of analyses. All of the numerical results are compared with those obtained by applying the Newmark explicit method. The examples and the simulation process on the Newmark explicit method were adopted from the examples in chapter 5.4 of Chopra's book [14]. The numerical programming tool employed was FORTRAN, and we developed the computation codes. The procedure of the calculation is shown in Fig. 4.

Figure 5(a) shows a plot of the displacement–force relationship for the positive stiffness case. Five stiffness segments are set using values k = 1, 2, 10, 2, and 1 [kip/in] from $-u$ to $+u$. The turning points of the displacements are given by $u = -2, -0.75, 0.75$, and 2 [in]. The associated equilibrium points are EQ″ = −8, EQ′ = −3, $\overline{\text{EQ}}' = 3$, and $\overline{\text{EQ}}'' = 8$. Figure 5(b) shows the displacement data, obtained from the PEM and the Newmark explicit method, around the turning point at u = 0.75 [in] (note k = 10 if $u < 0.75$, and k = 2 if $u > 0.75$), which is the first turning point after this model is triggered from zero. The time-steps in the Newmark explicit method are set as Δt = 0.05, 0.01, and 0.001 [sec]. The convergence trend from the Δt = 0.05 case to the Δt = 0.001 case is toward the exact case (marked by solid circles). Additionally, markers with extra circles represent data obtained by k = 10. These exceed the boundary of the displacement segment, which is sometimes termed "overshooting," and these small errors may propagate over repeated step-by-step iterations. These errors lead to instability in the calculations; most researchers apply extra iterative techniques to reduce overshooting. In this method, the turning point is obtained directly from the inverse function of the exact closed-form solution. The value of the time-step is not important here, because the closed-form solution is given.

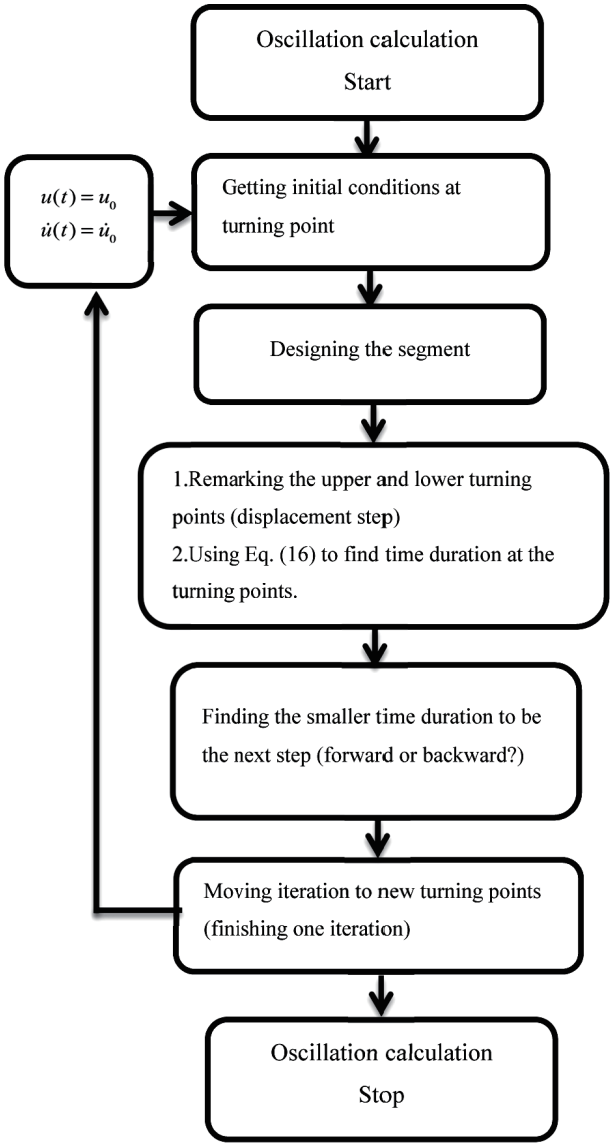
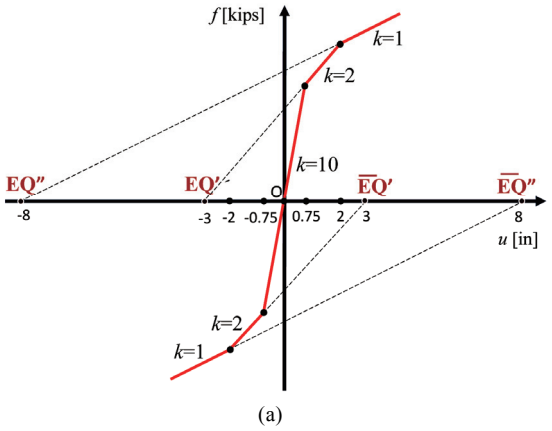


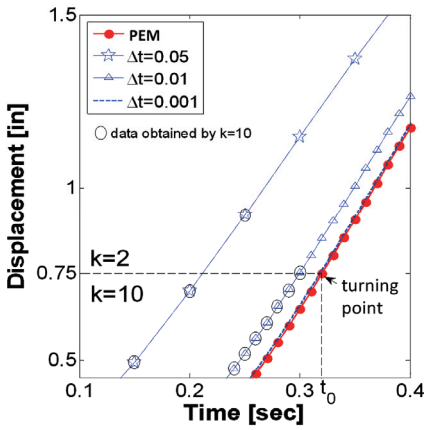
Fig. 4 The flow chart for the calculation procedure.

Figure 5(c) is the displacement history of the oscillation model for the first 6 [sec]. Time-steps are set as Δt = 0.1, 0.01, and 0.001 [sec] for the Newmark explicit method to show the numerical convergence. The time-step in the proposed method is Δt = 0.1, and the data follows the curve of the Δt = 0.001 case in the inset figure, showing the accuracy. The time-step in two methods (Δt = 0.1 and Δt = 0.001) has a maximum 100 times difference, but this doesn't imply a 99% time saving. Calculating the times at the turning points is the most time-consuming part of this method, and IMSL numerical library algorithm is applied. Time consumption depends on the accuracy of t_0, and this method has a roughly 60% time saving with errors less than 10^{-10}. Note that the sawtooth happened in the inserted figure is because the time-interval used in PEM is not enough to demonstrate the smooth curve. Since the advantage of the PEM is that proving the exact solutions in segments, choosing large or small time-intervals depends on the demonstration required.

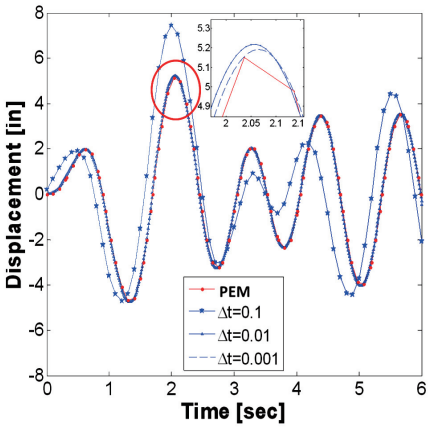
https://doi.org/10.1017/jmech.2014.83 Published online by Cambridge University Press



(a)

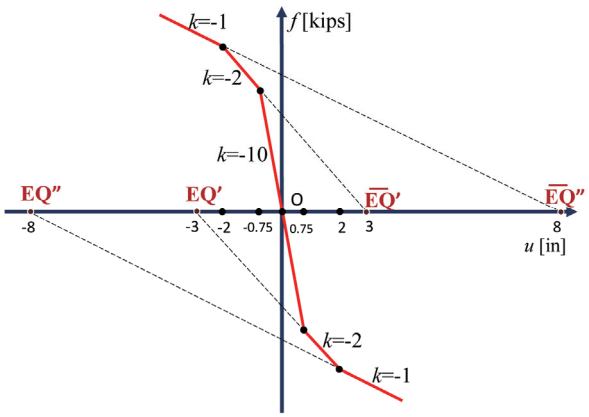


(b)

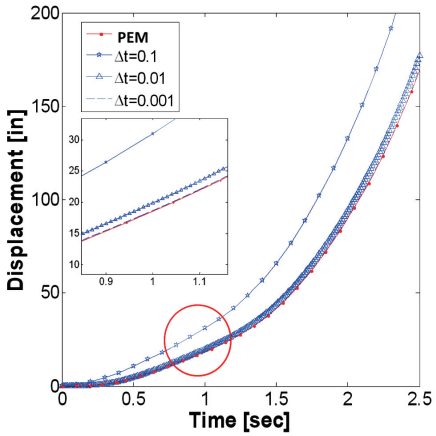


(c)

Fig. 5 (a) The displacement-force relationship for the positive stiffness case with equilibrium points is demonstrated. (b) Data around the first turning point obtained from the proposed method (PEM) compared with results from the Newmark explicit method (Δt = 0.05, 0.01, 0.001). Some data exceeding the boundary (overshooting; marked by extra circles) lead to instability of the calculation. (c) Displacement histories for two methods demonstrate convergence of various time-steps of the Newmark explicit method (Δt = 0.1, 0.01, 0.001) and the proposed method (PEM). The inset shows the proposed method with an even larger time-step while still obtaining accurate data.



(a)



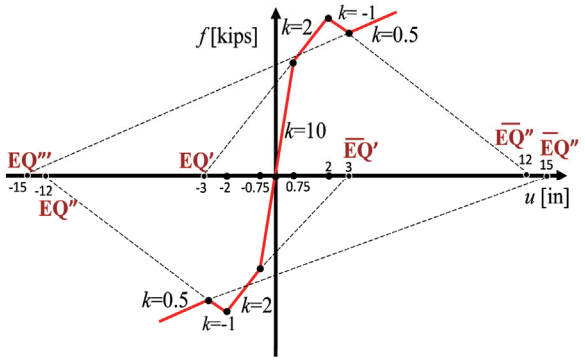
(b)

Fig. 6 (a) The displacement–force relation for the negative stiffness case with equilibrium points is demonstrated. (b) The displacement histories obtained from the two methods demonstrate convergence of various time-steps of the Newmark explicit method (Δt = 0.1, 0.01, 0.001) and the proposed method (PEM).

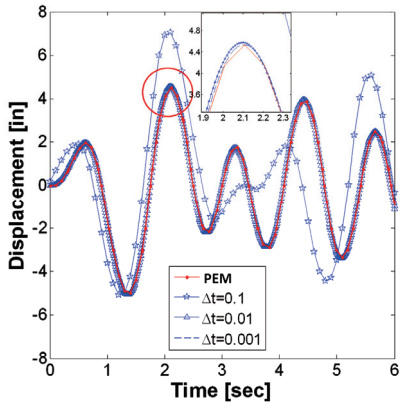
Figure 6(a) shows the graph of the displacement-force relationship for the negative stiffness case. Five stiffness segments are set by k = –1, –2, –10, –2, and –1 [kip/in] from $-u$ to $+u$. The turning points are given by u = –2, –0.75, 0.75, and 2 [in]. The associated equilibrium points are $\overline{EQ}'' = 8$, $\overline{EQ}' = 3$, EQ′ = –3, and EQ″ = –8. Figure 6(b) shows the displacement response for the first 2.5 [sec]. Various time-steps in the Newmark explicit method show a convergence trend. In the inset of the figure, the curve of this method (Δt = 0.1) coinciding with the results calculated with Δt = 0.001 in the Newmark explicit method indicates the accuracy of this method.

Figure 7(a) shows the graph of the displacement-force relationship for the mixed positive and negative stiffness case. Seven stiffness segments are chosen as k = 0.5, –1, 2, 10, 2, –1, and 0.5 [kip/in] from $-u$ to $+u$. The first and last stiffnesses of the model are set as positive to restrain the rigid block from diverging. The displacements at the turning points are u = –3, –2,

https://doi.org/10.1017/jmech.2014.83 Published online by Cambridge University Press



(a)



(b)

Fig. 7 (a) The displacement–force relation for the mixed positive and negative stiffness case with equilibrium points is demonstrated. (b) The displacement histories obtained from the two methods demonstrate convergence for various time-steps of the Newmark explicit method ($\Delta t = 0.1,\ 0.01,\ 0.001$) and the proposed method (PEM).

−0.75, 0.75, 2, and 3 [in]. The associated equilibrium points are $\overline{EQ}''' = 18$, $\overline{EQ}'' = 12$, $\overline{EQ}' = 3$, $EQ' = -3$, $EQ'' = -12$, and $EQ''' = -18$. Figure 7(b) shows the displacement histories for the first 6 [sec]. Various time-steps for the Newmark explicit method indicate a convergence trend. The time-step in this method is $\Delta t = 0.1$. The high accuracy of this method is demonstrated in the inset.

Generally speaking, the one who uses Newmark explicit method in solving dynamics has to consider the ratio between the natural frequency and the excitation frequency. It is an important issue to make sure the stability in the time step iteration and to reduce the error propagation. Fortunately, the PEM doesn't have to concern this ratio issue. Even the steps in PEM are not regular sizes, the PEM provides the exact solutions inside the steps and confirms the continuity at the turning points between steps. As a result, the natural frequency of the dynamic system or the frequency of the external force is not the issue to affect the accuracy of the solutions. Seriously speaking, we provide an analytical solution for the dynamic system, not a numerical solution. So short period or long period tests are the same, the results follow the certain equations, not iterations.

4. CONCLUSIONS

This paper introduced a new formulation of the PEMs to solve for the response of a single-degree-of-freedom system with nonlinear stiffness under a harmonic loading history. This method is characterized by providing the exact closed-form solution in each step, confirming continuity at the critical turning points between segments. Since the displacement-step replaces the time-step, which is the key iteration factor in traditionally numerical approximation methods, this method avoids the problems of instability and divergence induced by inappropriate selection of time-steps. The high accuracy and efficiency of the proposed method in comparison with the Newmark explicit method were demonstrated.

ACKNOWLEDGMENTS

The authors wish to thank the National Science Council of the Republic of China, Taiwan, for financial support under contracts NSC-101-2221-E-390-003.

REFERENCES

1. Clough, R. W. and Penzien, J., *Dynamics of Structures*, McGraw-Hill Inc., New York, U.S., pp. 111–131 (1993).
2. Liu, J. L., "Exact Solution for Dynamic Response of Multi-Degree-of-Freedom Bilinear Hysteretic System," *Journal of Engineering & Mechanics*, **129**, pp. 1342–1350 (2003).
3. Aydinoglu, M. N. and Fahjan, Y. M., "A Unified Formulation of the Piecewise Exact Method for Inelastic Seismic Demand Analysis Including the P-Delta Effect," *Earthquake Engineering & Structural Dynamics*, **32**, pp. 871–890 (2003).
4. Shih, P.-J. and Shih, W.-P., "Impact Dynamics of Vibratory Microprobe for Microcoordinate Measurement," *Journal Applied Physics*, **101**, p. 113516 (2007).
5. Shih, P.-J., "Tip-Jump Response of an Amplitude-Modulated Atomic Force Microscope," *Sensors*, **12**, pp. 6666–6684 (2012).
6. Newmark, N. M., "A Method of Computation for Structural Dynamics," *Journal of the Engineering Mechanics Division*, **85**, pp. 67–94 (1959).
7. Wilson, E. L., Farhoomand, I. and Bathe, K. J., "Nonlinear Dynamic Analysis of Complex Structures," *Earthquake Engineering & Structural Dynamics*, **1**, pp. 241–252 (1973).
8. Hughes, T. J. R., *The Finite Element Method-Linear Static and Dynamic Finite Element Analysis*, Prentice-Hall Inc., New Jersey, U.S. (1987).
9. Chang, S. Y., "A Technique for Overcoming Load Discontinuity in Using Newmark Method," *Journal*

https://doi.org/10.1017/jmech.2014.83 Published online by Cambridge University Press

of Sound and Vibration, **304**, pp. 556–569 (2007).
10. Chang, S. Y., "Accurate Integration of Nonlinear Systems Using Newmark Explicit Method," *Journal of Mechanical*, **25**, pp. 289–297 (2009).
11. Chang, S. Y., "Accurate Evaluation of Newmark Method Referring to Theoretical Solutions," *Journal of Earthquake Engineering*, **12**, pp. 1–16 (2008).
12. Hilber, H. M., Hughes, Thomas J. R. and Taylor, R. L., "Improved Numerical Dissipation for Time Integration Algorithms in Structural Dynamics," *Earthquake Engineering & Structural Dynamics*, **5**, pp. 283–292 (1977).
13. Bathe, K. J. and Irfan Baig, M. M., "On a Composite Implicit Time Integration Procedure for Nonlinear Dynamics," *Computers & Structures*, **83**, pp. 2513–2524 (2005).
14. Chopra, A. K., *Dynamics of Structures: Theory and Applications to Earthquake Engineering*, 3rd Edition, Prentice Hall, Englewood Cliffs, New Jersey, U.S. (2012).

(Manuscript received January 20, 2014,
accepted for publication June 25, 2014.)

https://doi.org/10.1017/jmech.2014.83 Published online by Cambridge University Press